

Article

# Antiproliferative Activity of Combined Biochanin A and Ginsenoside Rh<sub>2</sub> on MDA-MB-231 and MCF-7 Human Breast Cancer Cells

Guixing Ren <sup>1</sup>, Zhenxing Shi <sup>2</sup>, Cong Teng <sup>3</sup> and Yang Yao <sup>3,\*</sup>

<sup>1</sup> College of Pharmacy and Biological Engineering, Chengdu University, No.1 Shilling Road, Chenglo Avenue, Longquan District, Chengdu 610106, China; guixin@126.com

<sup>2</sup> Laboratory of Biomass and Green Technologies, University of Liege-Gembloux Agro-Bio Tech, Passage des Déportés 2, B-5030 Gembloux, Belgium; zhenxing@126.com

<sup>3</sup> Institute of Crop Science, Chinese Academy of Agricultural Sciences, No.80 South Xueyuan Road, Haidian District, Beijing 100081, China; 82101172124@caas.cn

\* Correspondence: yaoyang@caas.cn; Tel.: +86-10-621-155-95

Received: 8 October 2018; Accepted: 3 November 2018; Published: 8 November 2018



**Abstract:** Breast cancer is the most frequently diagnosed cancer in women worldwide. The antiproliferative activities of biochanin A (BA) and ginsenoside Rh<sub>2</sub> were determined by evaluating their inhibitory effect on MDA-MB-231 human breast cancer cell proliferation. The combination of BA with Rh<sub>2</sub> was also assessed. In MDA cells, combination treatment led to a decrease in the EC<sub>50</sub> values of BA and Rh<sub>2</sub> to 25.20 μM and 22.75 μM, respectively. In MCF-7 cells, the EC<sub>50</sub> values of combined BA and Rh<sub>2</sub> decreased to 27.68 μM and 25.41 μM, respectively. BA combined with Rh<sub>2</sub> also improved the inhibition of MDA-MB-231 and MCF-7 cell migration and invasion compared to the individual compounds. Western blot analysis demonstrated upregulation in p-p53, p-p38, and p-ASK1 proteins while levels of TRAF2 were downregulated. These results suggest that BA combined with Rh<sub>2</sub> exhibits synergistic effects against MDA-MB-231 and MCF-7 cell proliferation.

**Keywords:** synergy; biochanin A; Rh<sub>2</sub>; breast cancer; antiproliferative activity

## 1. Introduction

Today, breast cancer is the second leading cause of mortality in women worldwide. More than two hundred thousand new breast cancer cases were diagnosed in the United States in 2016 according to epidemiology, surveillance, and the end result program [seer.cancer.gov](http://seer.cancer.gov) [1]. Triple negative breast cancer is characterized by tumors that are human epidermal growth factor receptor 2-negative, progesterone receptor-negative, and estrogen receptor-negative [2]. MDA-MB-231 and MCF-7 human cancer cell lines are estrogen receptor and estrogen receptor-positive cells, respectively. These cell lines are well-established in vitro models for evaluating estrogen-responsive or estrogen-independent antineoplastic drugs [3].

Numerous studies have shown that natural products play an important role in the inhibition and therapy of cancers [4]. The nutritional function of food shows the synergistic and additive effects of phytochemicals compared to a single compound [5]. Differences in solubility, polarity, and molecular size of these compounds can affect their distribution and bioavailability in various organs, tissues, cells, and subcellular organelles. Furthermore, purified phytochemicals may lose some of their bioactivity and behave differently than in whole foods [6]. Similarly, chemotherapeutic combinatorial methods have been conducted to decrease drug side effects, slow the growth of cancer cells, and achieve results superior to those of one active drug alone.

Biochanin A (BA), an isoflavone, has been shown to possess antiviral [7], antioxidant [8], anticarcinogenic [9], anti-inflammatory [10], and protective effects on endothelial integrity and function [11]. BA exhibits promise as a phytochemical driving the inhibition of breast cancer through promoting estrogen receptor-positive cell proliferation [12]. Rh<sub>2</sub> (protopanaxadiol-type) is the major dammarane-type saponin ginsenoside. Previous studies have shown that Rh<sub>2</sub> has beneficial impacts against breast cancer [13], hepatoma cells [14], glioma cells [15], prostate cancer cells [16], and lung cancer cells [17]. Previous publications describe the interactions between isoflavone and ginseng saponins and their role in suppressing MDA-MB-231 cell proliferation. The aim of this study was to determine whether BA and Rh<sub>2</sub> have additive and/or synergistic effects on MDA-MB-231 and MCF-7 human breast cancer cell proliferation.

## 2. Results and Discussion

### 2.1. Cytotoxicity and Antiproliferative Activities of MDA-MB-231 and MCF-7

BA and Rh<sub>2</sub> both show no cytotoxicity at doses of 10–100  $\mu\text{M}$  (data not shown). These data is supported by previous work performed by Tan and Kim reporting that 100  $\mu\text{M}$  BA had no toxic effects in PC12 cells [18]. Furthermore, Quan's studies have shown that Rh<sub>2</sub> at 80  $\mu\text{M}$  dose exhibited no cytotoxic activity in the cells [19]. The antiproliferative effects of BA, Rh<sub>2</sub>, and the combination of BA with Rh<sub>2</sub> on cell growth are presented in Figure 1. BA, at doses of 30–70  $\mu\text{M}$  ( $p < 0.05$ ), shows dose-dependent antiproliferative effects on MDA-MB-231 and MCF-7 cell growth (Figure 1A,B). The EC<sub>50</sub> values of BA in inhibiting the growth of MDA-MB-231 and MCF-7 were 63.76  $\mu\text{M}$  and 59.76  $\mu\text{M}$ , respectively. Rh<sub>2</sub> also showed a dose-dependent prevention of proliferation in both cell lines at doses of 30–70  $\mu\text{M}$  (Figure 1A,B). The EC<sub>50</sub> values of Rh<sub>2</sub> in inhibiting MDA-MB-231 and MCF-7 cell line proliferation were 57.53  $\mu\text{M}$  and 52.53  $\mu\text{M}$ , respectively (Table 1).

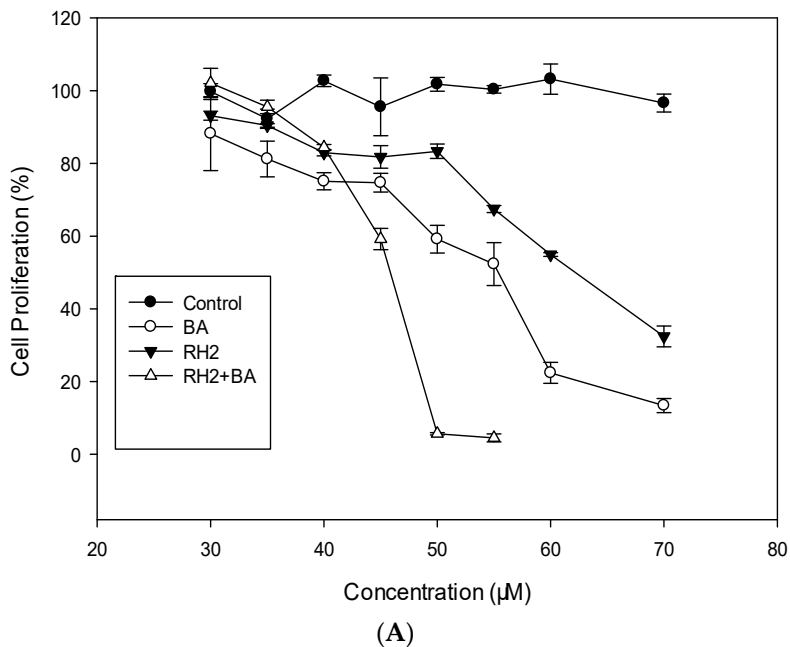
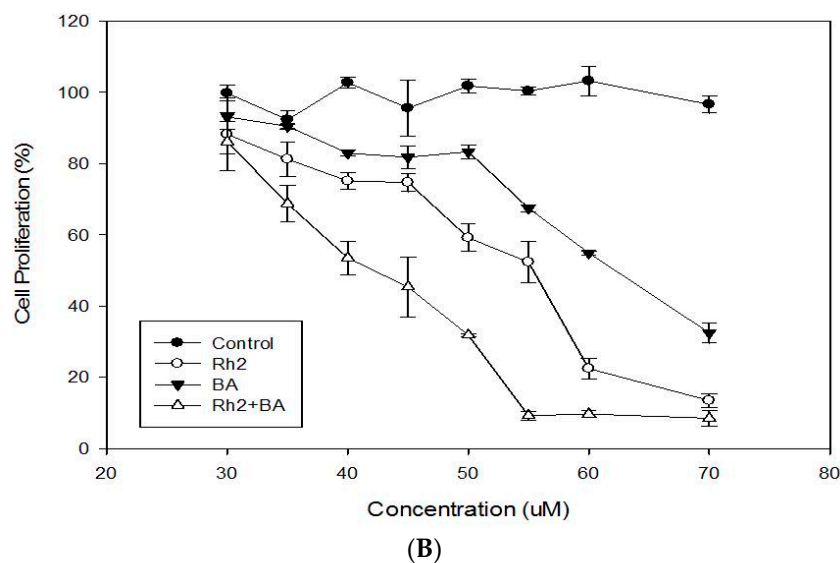


Figure 1. Cont.



**Figure 1.** Antiproliferative effects of BA, Rh<sub>2</sub>, and the combination of BA with Rh<sub>2</sub> on MDA (A) and MCF-7 (B) human breast cancer cell lines (mean  $\pm$  SD,  $n = 3$ ). Each value represents the mean  $\pm$  SD of triplicate biological experiments.

**Table 1.** The EC<sub>50</sub> values of BA and Rh<sub>2</sub> towards MDA-MB-231 and MCF-7 cells.

Component	EC <sub>50</sub> Value			
	MDA-MB-231		MCF-7	
	Single	Combined	Single	Combined
Biochanin A	63.76 $\mu$ M	25.20 $\mu$ M	59.76 $\mu$ M	27.68 $\mu$ M
Rh <sub>2</sub>	57.53 $\mu$ M	22.75 $\mu$ M	52.53 $\mu$ M	25.41 $\mu$ M

Tsu et al. reported that BA concentrations exceeding 30  $\mu$ g/mL in MCF-7 cells exhibited dose-dependent effects on cell proliferation. At 100  $\mu$ g/mL, MCF-7 cell proliferation was attenuated by approximately 80% [20]. Moon et al. demonstrated a role for BA in breast cancer prevention using xenograft mouse models. In this study, BA treatment groups (5 mg/kg) had significantly inhibited growth of tumors compared to the control group [21]. Choi et al. showed that Rh<sub>2</sub> treatment inhibited the viability of MDA-MB-231 cells by 28% and 85% at doses of 40  $\mu$ M and 60  $\mu$ M, respectively [22].

Drug combinations have received increasing attention due to the advantages of lower drug doses, reduced side effects, and improved anticancer effects. Data in Figure 1 suggest that the combination of Rh<sub>2</sub> plus BA significantly increased the antiproliferative activity of cells compared to the effects of Rh<sub>2</sub> or BA alone. In MDA-MB-231 cells, the EC<sub>50</sub> values of combined BA and Rh<sub>2</sub> were decreased to 25.20  $\mu$ M and 22.75  $\mu$ M, respectively, which represents 2.53-fold and 2.52-fold less than those of BA and Rh<sub>2</sub> alone. In MCF-7 cells, the EC<sub>50</sub> values of combined BA and Rh<sub>2</sub> were decreased to 27.68  $\mu$ M and 25.41  $\mu$ M, respectively, which were 2.16-fold and 2.07-fold less than those of BA and Rh<sub>2</sub> alone. At 50, 75, 90, and 95% inhibition of cell growth, the CI numbers of the combined BA and Rh<sub>2</sub> treatment were  $0.42 \pm 0.05$ ,  $0.55 \pm 0.09$ ,  $0.72 \pm 0.11$ , and  $0.88 \pm 0.10$ , respectively, suggesting that considerable synergistic effects exist at all tested doses (Table 2).

**Table 2.** The CI numbers of combined BA and Rh<sub>2</sub>.

CI Values at Different Inhibition of Rates			
50%	75%	90%	95%
0.435	0.553	0.723	0.882

Moon et al. compared the co-administration of quercetin, epigallocatechin-3-gallate, and BA with the administration of BA alone in a murine xenograft model. The results showed that combined BA, quercetin, and epigallocatechin-3-gallate (5 mg/kg) led to improved efficacy comparable to that of 15 mg/kg BA alone [21]. This could be in part due to the fact that the combination of BA, quercetin, and epigallocatechin-3-gallate causes improved oral bioavailability of BA in animal models. The combination significantly increases the level of BA in plasma samples after either oral administration or intravenous injection. Oral bioavailability was improved three-fold compared to the administration of BA alone [23]. Xie et al. evaluated the synergistic effect of Rh<sub>2</sub> plus paclitaxel on LNCaP prostate cancer models both in vitro and in vivo. The data suggested that Rh<sub>2</sub> plus paclitaxel exhibit synergy in LNCaP cells at less than 50% of the effective dose values. The combination of Rh<sub>2</sub> and paclitaxel resulted in a significant reduction of prostate specific antigen in serum, and inhibition in the growth of LNCaP tumors. In addition, immunohistochemistry results showed obvious effects on proliferation agents [24].

## 2.2. Enhanced Inhibition of Cell Migration

Tumor cell migration and invasion are the two most important traits of metastasis. To further study the inhibitory roles of BA, Rh<sub>2</sub>, and BA combined with Rh<sub>2</sub> on metastasis, we evaluated their effect on cell migration and invasion. A wound-healing assay was used to evaluate the inhibition of BA, Rh<sub>2</sub>, and BA with Rh<sub>2</sub> on cell migration. Both BA and Rh<sub>2</sub> inhibited wound closure in MDA-MB-231 and MCF-7 cells (Figure 2A,C). In MDA cells, the combination of BA plus Rh<sub>2</sub> significantly enhanced the inhibition compared to Rh<sub>2</sub> alone. The combination treatment inhibited wound closure by 39% and 29% compared to that of the control in MDA-MB-231 and MCF-7 cells, respectively (Figure 2B,D).

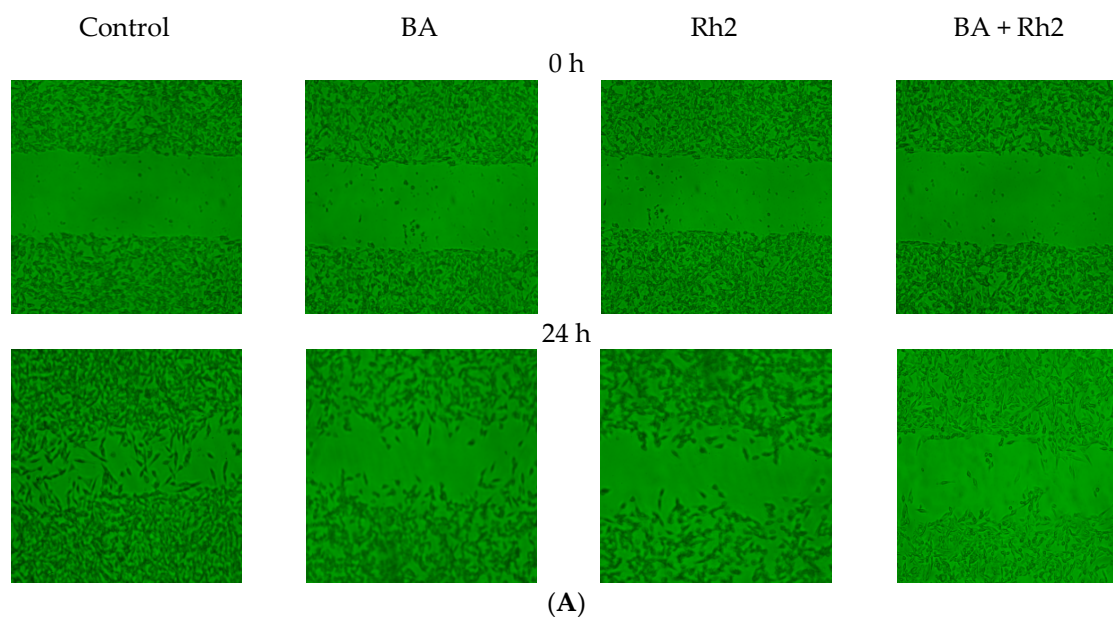


Figure 2. Cont.

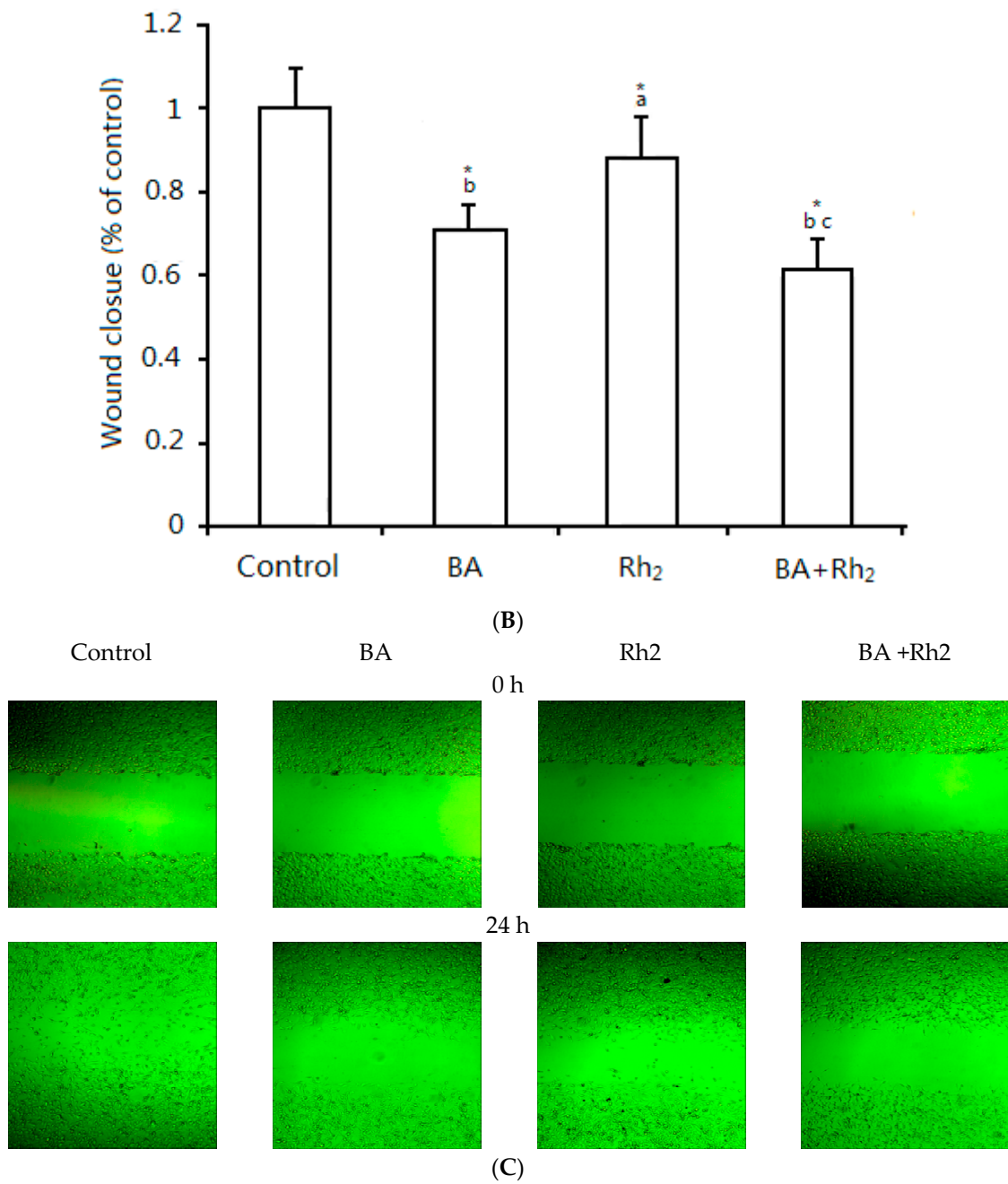
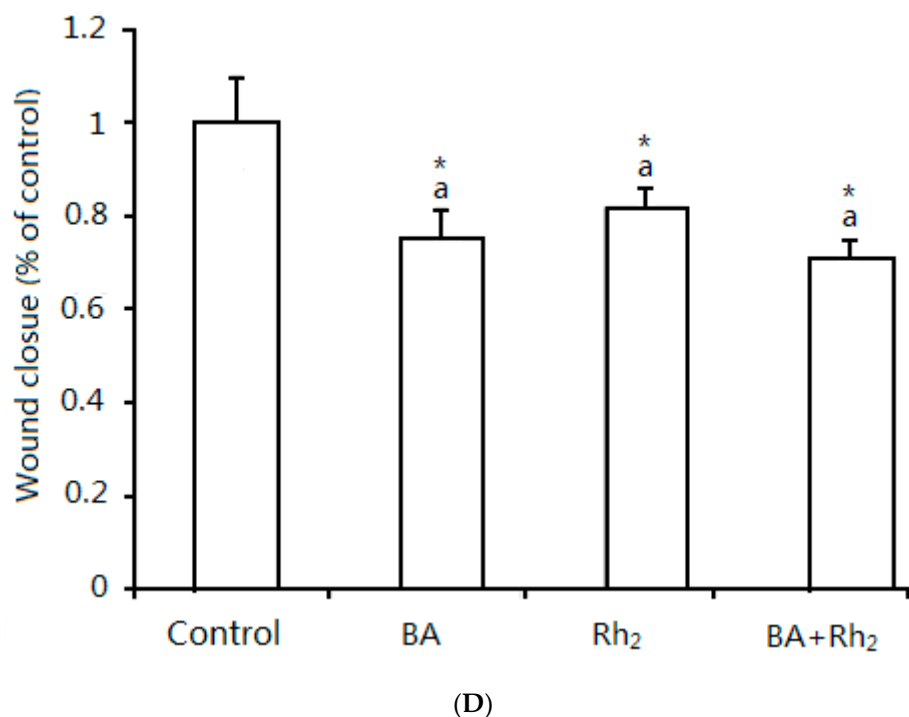
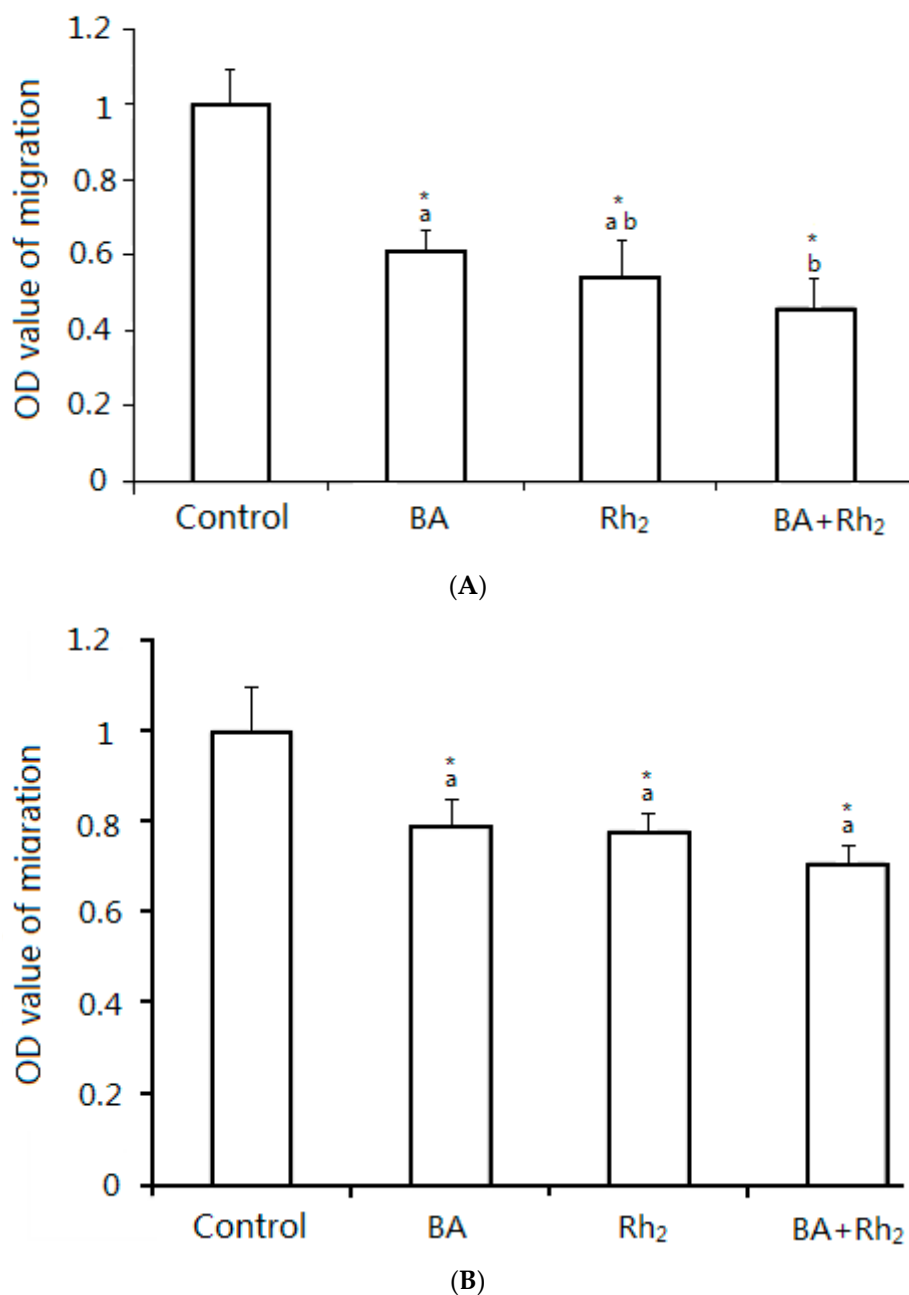


Figure 2. Cont.



**Figure 2.** For the scratch assay, wounds were made when MDA (A,B) and MCF-7 (C,D) cells were 90–100% confluent and after an overnight starvation. Cells were treated with vehicle control, 63.76  $\mu$ M BA, 57.53  $\mu$ M Rh<sub>2</sub>, or 25.20  $\mu$ M BA + 22.75  $\mu$ M Rh<sub>2</sub> for 24 h. The closure of wounds was imaged and measured at 0 and 24 h. An asterisk (\*) indicates a significant difference from the control ( $p < 0.05$ ). \* Compared to the control,  $p < 0.05$ . Different letters showed significant difference in sample groups ( $p < 0.05$ ).

To measure the effect of BA, Rh<sub>2</sub>, and BA plus Rh<sub>2</sub> on cell invasion we used a trans-well chamber assay. The mixture of BA plus Rh<sub>2</sub> increased the inhibition in both cell lines compared to BA or Rh<sub>2</sub> alone (Figure 3A,B). In MDA cells, the BA plus Rh<sub>2</sub> significantly increased inhibition compared to BA. Migration of MDA-MB-231 and MCF-7 cells was separately inhibited by 57% and 29% under combined BA and Rh<sub>2</sub> treatment compared to the control. In summary, these results indicate that BA, Rh<sub>2</sub>, and BA plus Rh<sub>2</sub> exert strong inhibition activities on the migration and invasion of triple-negative breast cancer cells. Additionally, the combination exhibited greater effectiveness in these two assays.



**Figure 3.** In the trans-well chamber assay, MDA (A) and MCF-7 (B) cells were treated with vehicle control, EC<sub>50</sub> values of BA, Rh<sub>2</sub> and BA with Rh<sub>2</sub> for 48 h. Cells suspended in serum-free media were seeded on the upper membrane of the trans-well chamber and incubated for 48 h. Complete growth medium was added on the bottom. Cells on the lower membrane of the chambers were counted. Data are presented as mean  $\pm$  SD. An asterisk (\*) indicates a significant difference from the control ( $p < 0.05$ ). \* Compared to the control,  $p < 0.05$ . Different letters showed significant difference in sample groups ( $p < 0.05$ ).

Xiao et al. showed that BA exhibits anticancer effects by evaluating the migratory effect of BA on wound healing and invasion in SK-Mel-28 human malignant melanoma cells. They observe that treatment with 0, 10, 50 and 100  $\mu$ M doses of BA result in the suppression of migration and invasion in a dose-dependent manner [25].

### 2.3. Modulations of Protein Expression and Signalling Pathways

The regulation of protein expression and signaling pathways in MDA-MB-231 and MCF-7 cells were similar (Figure 4). BA demonstrated considerable capabilities in the upregulation of phosphorylated p53



(p-p53) and phosphorylated p38 (p-p38) protein levels relative to Rh<sub>2</sub> (Figure 4A,B,E,F). The inhibitory effects were further improved by BA and Rh<sub>2</sub> combination. Cell growth, apoptosis and cycle progression are regulated by p38 MAPK [26]. Expression of phosphorylated apoptosis signal-regulating kinase 1 (p-ASK1) was significantly enhanced after treatment with the BA plus Rh<sub>2</sub> combination compared to the control (Figure 4C,G). However, the combination of BA and Rh<sub>2</sub> significantly downregulated the protein expression of TNF receptor associated factor 2 (TRAF2), which serves as a mediator of the anti-apoptotic marker (Figure 4D,H). Upregulated p-ASK1 and downregulated TRAF2 promote the kinase p38 pathway, resulting in the phosphorylation of p53 and thus triggering anti-proliferation and apoptosis in cells [27].

Liu et al. evaluated the proliferative effect of Rh<sub>2</sub> in KG1- $\alpha$  and K562 human leukemia cells in vitro and the inhibitory effect on the growth of human leukemia xenograft tumors in vivo. The data showed that Rh<sub>2</sub> exerts antiproliferative effects on those cells by increasing histone acetylation. In addition, Rh<sub>2</sub> significantly modulated JNK, p-JNK, p38, and p-p38 protein expression thus inducing apoptosis by activating the MAPK signaling pathway [28]. Choi et al. observed that Rh<sub>2</sub> inhibits MDA-MB-231 cell viability by reducing the contents of phosphorylated retinoblastoma protein and lowering the transcriptional activity of E2 promoter binding factor 1, as shown by the luciferase reporter assay. In addition, Rh<sub>2</sub> regulated cyclin-dependent kinases (Cdk), cyclins, and the cell cycle, resulting in induced interaction between Cdk4/Cdk6 and cyclin D1, as well as improved recruitment of p15Ink4B and p27Kip1 to cyclin D1/Cdk4 and cyclin D1/Cdk6 complexes [22]. It has also been reported that Rh<sub>2</sub> induces apoptotic cell death by triggering caspase-1 and caspase-3, and upregulating Bax in neuroblastoma cells [29]. Ginsenoside Rg5 promotes breast cancer cell apoptosis by inducing G0/G1 cell cycle arrest in MCF-7 and MDA-MB-453 human breast cancer cell lines. P53-dependent apoptosis indicates that the tumor inhibitor p53 induces cell self-destruction through the endogenous mitochondrial and exogenous death receptor pathways [30]. Thus, p53-dependent apoptosis could be used to lead to the expression of proapoptotic members. If cells undergo DNA damage, p53 arrests the cell cycle by p21 or by induction of apoptosis. To respond to DNA damage or cellular stress, p53 is stabilized by post-transcriptional modifications, and the concentration of p53 increases [31]. Stabilization and activation of p53 is responsible for cellular antiproliferative mechanisms, such as growth arrest, cell senescence, and apoptosis [32].



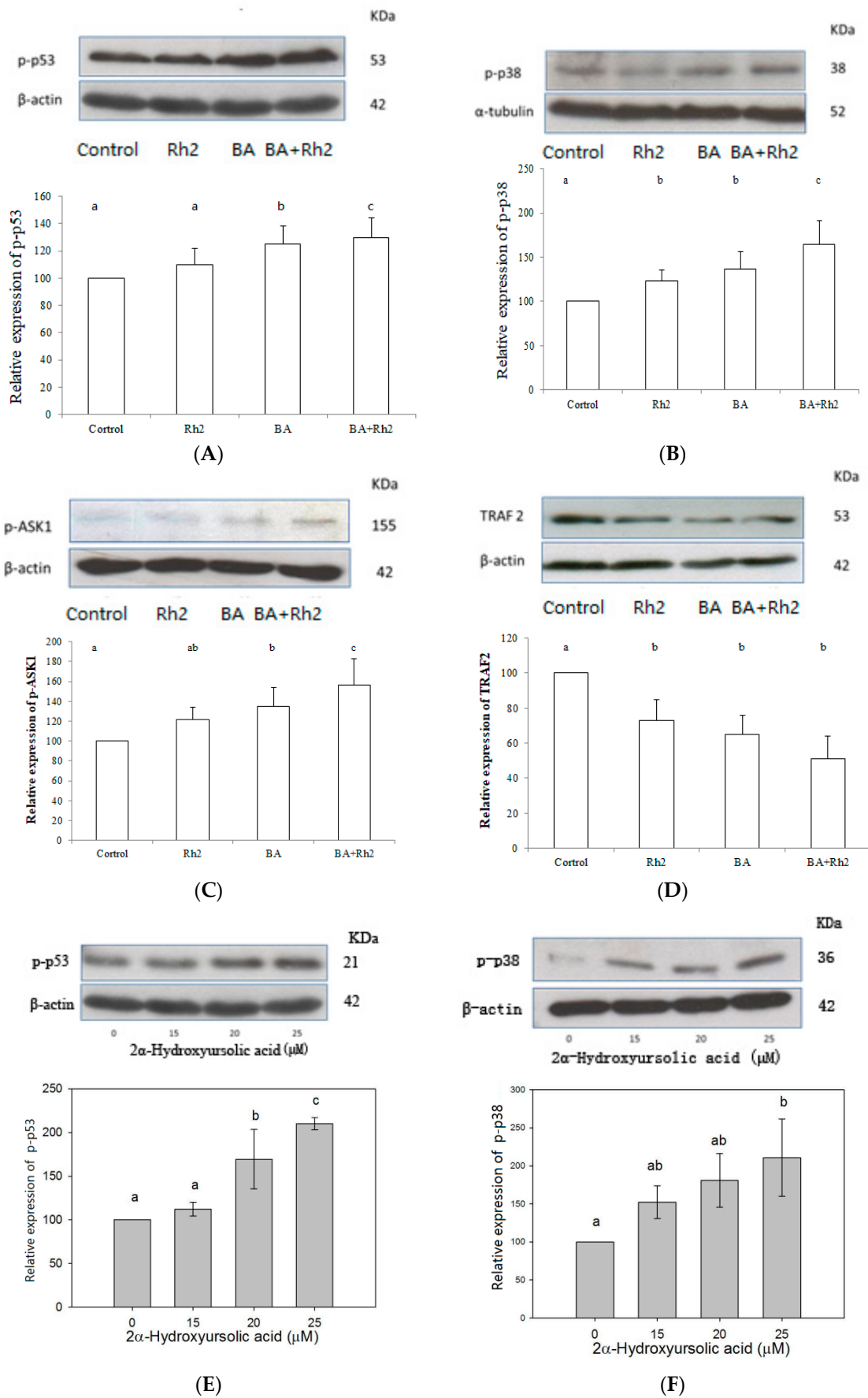
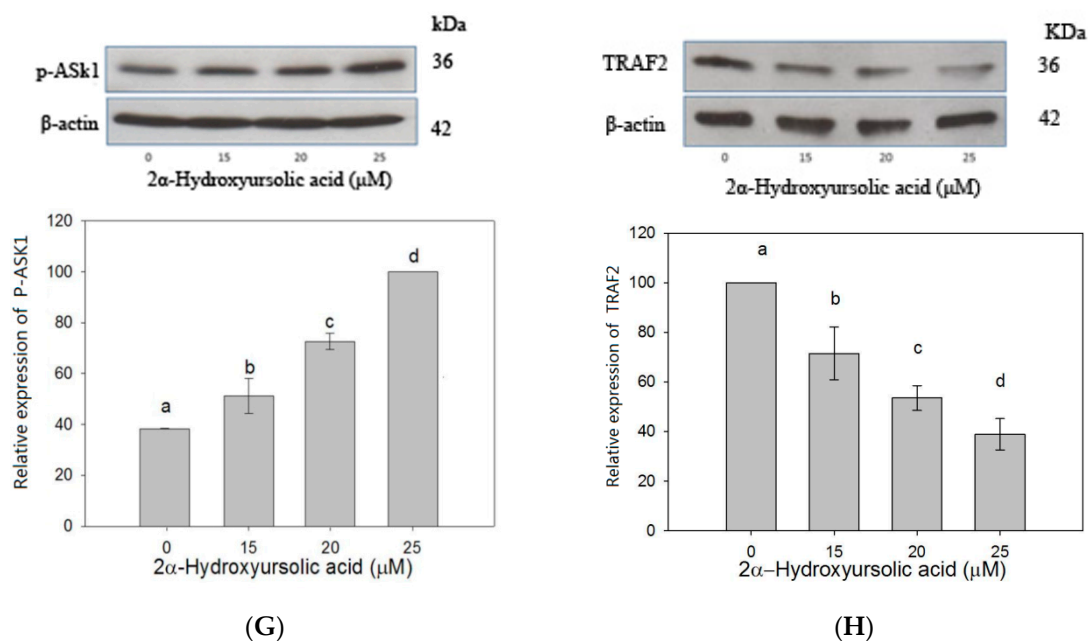


Figure 4. Cont.



**Figure 4.** Effects of BA, Rh<sub>2</sub> and the combination of BA and Rh<sub>2</sub> on expression of p-p53 (A,E), p-p38 (B,F), p-ASK1 (C,G), and TRAF 2 (D,H) in MDA-MB-231 and MCF-7 human breast cancer cells. Bars with no letters in common are significantly different ( $p < 0.05$ ). Each value represents the mean  $\pm$  SD of triplicates. Different letters showed significant difference in sample groups ( $p < 0.05$ ).

### 3. Materials and Methods

#### 3.1. Chemicals

Rh<sub>2</sub> and BA were purchased from the National Institutes for Food and Drug Control (Beijing, China). MDA-MB-231 human breast cancer cells were purchased from the American Type Culture Collection (Manassas, VA, USA). Fetal bovine serum,  $\alpha$ -minimum essential medium ( $\alpha$ -MEM), Hank's Balanced Salt Solution (HBSS), 2-(4-(2-hydroxyethyl)-1-piperazinyl)-ethanesulfonic acid (HEPES) and phosphate-buffered saline (PBS) were purchased from Gibco Life Technologies (Grand Island, NY, USA). Methylene blue and dimethyl sulfoxide (DMSO) were purchased from Sigma-Aldrich (St. Louis, MO, USA). Extracellular matrix (ECM) invasion assay kits were purchased from Millipore (Billerica, MA, USA).

#### 3.2. Cytotoxicity Activity

The cytotoxicity of Rh<sub>2</sub> or BA towards MDA-MB-231 cells and MCF-7 cells was evaluated by methylene blue assay as reported previously [33]. In brief, MDA-MB-231 cells were cultured in  $\alpha$ -MEM containing 10 mM HEPES, 1% antibiotic-antimycotic and 10% fetal bovine serum. MCF-7 cells were maintained in  $\alpha$ -MEM containing 10 mM HEPES, 1% antibiotic-antimycotic, 0.01 mg/mL insulin, and 10% fetal bovine serum as described previously [34]. MDA-MB-231 and MCF-7 cells were maintained in an incubator at 5% CO<sub>2</sub> and 37 °C. A total of  $5 \times 10^4$  cancer cells in growth media were placed in each well of a 96-well flat-bottom plate. After that, the growth medium was changed to include the treatments or 100  $\mu$ L new medium as control. After 24 h of incubation, cells were rinsed with phosphate-buffered saline. Cells were then stained with methylene blue solution (0.6% methylene blue, 0.67% glutaraldehyde, and 98% HBSS) and incubated for 1 h. The solution was removed and washed with deionized water. After the wells were dried, methylene blue was stained in cells with the elution buffer (50% ethanol, 49% PBS, and 1% acetic acid) and rotated for 15 min. The absorbance was read at 570 nm by using a microplate reader (Bio-Rad, Danvers, MA, USA). Cytotoxicity was evaluated as a percentage compared to the control.

### 3.3. Antiproliferative Activity

The antiproliferative activities of Rh<sub>2</sub> and BA towards MDA-MB-231 cells and MCF-7 cells were measured by the methylene blue assay [24]. MDA-MB-231 cells and MCF-7 cells were incubated in the same conditions described above. The cells were seeded at  $2.5 \times 10^6$  cells/mL, and various concentrations of Rh<sub>2</sub>, BA, or control were added to the cells. After 72 h, cell proliferation was determined using the methylene blue assay measuring absorbance at 570 nm.

### 3.4. Combination Study

A study on the combination of Rh<sub>2</sub> and BA towards MDA-MB-231 and MCF-7 cell proliferation was designed. The EC<sub>50</sub> values of Rh<sub>2</sub> and BA were evaluated according to dose-response curves. The combination concentrations of Rh<sub>2</sub> and BA were  $0.125 \times EC_{50}$ ,  $0.25 \times EC_{50}$ ,  $0.50 \times EC_{50}$ ,  $0.75 \times EC_{50}$ ,  $1.00 \times EC_{50}$ , and  $1.25 \times EC_{50}$ , respectively. Finally, a series of concentrations of Rh<sub>2</sub> and BA were mixed to generate the dose-response curve in the MDA-MB-231 and MCF-7 cell proliferation models. A combination index (CI) was calculated for the combinations of Rh<sub>2</sub> and BA using the Compu Syn software (ComboSyn, Inc., Paramus, NJ, USA), on account of the mass-action law and Chou–Talalay equation [35]. A value of CI below 1 indicates a synergistic effect of a combination, equal to 1 shows additive effects, and higher than 1 indicates antagonistic effects.

### 3.5. Wound-Healing Assay

A wound closure seeding model was built using silicon culture inserts (Ibidi, LLC, Munchen, Germany) with two individual wells for cell seeding. The insert was placed in a culture dish, and  $5 \times 10^5$  cells/mL of MDA-MB-231 and MCF-7 cells were plated in each well and grown to form a confluent and homogeneous layer. The culture insert was removed, and a cell-free area was recorded after 24 h cell seeding. The wound was approximately 500  $\mu$ m wide. Healing of the wound by migrating cells after Rh<sub>2</sub>, BA or Rh<sub>2</sub> plus BA treatment was observed after 24 h by light microscopy (CX-2, Olympus) and analyzed using Image J software (NIH, Bethesda, Maryland, USA) [36].

### 3.6. Invasion Assay

An ECM kit assay was used to evaluate cell invasiveness. According to the manufacturer's protocols,  $5 \times 10^5$  cells were suspended in 300  $\mu$ L of serum-free media and plated on an ECM-coated membrane insert. The invasion assay was examined after 48 h of control, Rh<sub>2</sub>, BA or Rh<sub>2</sub> combined with BA treatment. After that, the cells in the upper insert were wiped away, while the cells on the lower side were stained [37].

### 3.7. Western Blot Analysis

Western blot analysis was conducted according to the method of Yao et al. [38]. The supernatant was collected after lysed cells were centrifuged at 12,000 rpm at 4 °C for 15 min. Protein extracts were separated with SDS-PAGE and transferred to PVDF membrane. After blocking, p-p53, p-p38, p-ASK1, TRAF2, and  $\beta$ -actin antibodies (Santa Cruz Biotechnology, Santa Cruz, CA, USA) were added and incubated. Membranes were washed and incubated in PBST and HRP-conjugated secondary antibody, respectively. The signals were detected using the Super Signal ELISA Pico Chemiluminescent Substrate (Thermo Fisher Scientific, Waltham, MA, USA).

### 3.8. Statistical Analysis

Data were analyzed using Sigma Plot software version 11.0 (Systat Software, Inc., Chicago, IL, USA). All values were expressed as the means  $\pm$  SD of at least three independently performed experiments. Statistical analyses were conducted with Student's *t*-test and analysis of variance (ANOVA) by SPSS software version 16.0. Differences with  $p < 0.05$  were considered to be statistically significant.

#### 4. Conclusions

In summary, a novel combinatorial treatment with BA plus Rh2 synergistically enhanced the antiproliferative effect in MDA-MB-231 and MCF-7 cells and was associated with the upregulated expression of p-p53, p-p38, and p-ASK1 and downregulated expression of TRAF2. Further in vivo studies are necessary to verify the efficacy and appropriate doses of the combination for alleviating receptor 2-negative, progesterone receptor-negative, and estrogen receptor-negative breast cancer in clinical trials.

**Author Contributions:** Conceptualization, G.R. and Y.Y.; methodology, C.T. and Z.S.; software, Z.S.; validation Z.S. and Y.Y.; formal analysis, Z.S.; data curation, C.T.; writing—original draft preparation, G.R.; writing—Z.S. and editing, Y.Y.; visualization, supervision, G.R.; project administration, Y.Y.; funding acquisition, G.R.

**Funding:** This work was supported by China Agriculture Research System (CARS-080G20) and the Agricultural Science and Technology Innovation Program (CAAS-ASTIP-2017-ICS).

**Conflicts of Interest:** The authors declare no conflict of interest and the funders had no role in the design of the study; in the collection, analyses, or interpretation of data; in the writing of the manuscript, or in the decision to publish the results.

#### References

1. Dutta, P.; Sarkissyan, M.; Paico, K.; Wu, Y.Y.; Vadgama, J.V. MCP-1 is overexpressed in triple-negative breast cancers and drives cancer invasiveness and metastasis. *Breast Cancer Res. Treat.* **2018**, *3*, 477–486. [[CrossRef](#)] [[PubMed](#)]
2. Kreike, B.; van Kouwenhove, M.; Horlings, H.; Weigelt, B.; Peterse, H.; Bartelink, H.; van de Vijver, M.J. Gene expression profiling and histopathological characterization of triple-negative/basal-like breast carcinomas. *Breast Cancer Res.* **2007**, *9*, R65. [[CrossRef](#)] [[PubMed](#)]
3. Kaushik, S.; Shyam, H.; Sharma, R.; Balapure, A.K. Genistein synergizes centchroman action in human breast cancer cells. *Indian J. Pharmacol.* **2016**, *48*, 637. [[PubMed](#)]
4. Gan, D.; Zeng, X.; Liu, R.H.; Ye, H. Potential mechanism of mycelium polysaccharide from *pholiota dinghuensis* bi in regulating the proliferation and apoptosis of human breast cancer mcf-7 cells through p38/mapk pathway. *J. Funct. Foods* **2015**, *12*, 375–388. [[CrossRef](#)]
5. Liu, R.H. Potential synergy of phytochemicals in cancer prevention: Mechanism of action. *J. Nutr.* **2004**, *134*, 3479–3485. [[CrossRef](#)] [[PubMed](#)]
6. Yang, J.; Liu, R. HSynergistic effect of apple extracts and quercetin 3-beta-d-glucoside combination on antiproliferative activity in MCF-7 human breast cancer cells in vitro. *J. Agric. Food Chem.* **2009**, *57*, 8581–8586. [[CrossRef](#)] [[PubMed](#)]
7. Cirone, M.; Zompetta, C.; Tarasi, D.; Frati, L.; Faggioni, A. Infection of human T lymphoid cells by human herpesvirus 6 is blocked by two unrelated protein tyrosine kinase inhibitors, biochanin A and herbimycin. *AIDS Res. Hum. Retrovir.* **1996**, *12*, 1629–1634. [[CrossRef](#)] [[PubMed](#)]
8. Rufer, C.E.; Kulling, S.E. Antioxidant activity of isoflavones and their major metabolites using different in vitro assays. *J. Agric. Food Chem.* **2006**, *54*, 2926–2931. [[CrossRef](#)] [[PubMed](#)]
9. Puli, S.; Lai, J.C.; Bhushan, A. Inhibition of matrix degrading enzymes and invasion in human glioblastoma (U87MG) cells by isoflavones. *J. Neurooncol.* **2006**, *79*, 135–142. [[CrossRef](#)] [[PubMed](#)]
10. Kalayciyan, A. Nicotine and biochanin A, but not cigarette smoke, induce anti-inflammatory effects on keratinocytes and endothelial cells in patients with Behcet’s disease. *J. Investig. Dermatol.* **2007**, *127*, 81–89. [[CrossRef](#)] [[PubMed](#)]
11. Schrepfer, S. The selective estrogen receptor-beta agonist biochanin A shows vasculo protective effects without uterotrophic activity. *Menopause* **2006**, *13*, 489–499. [[CrossRef](#)] [[PubMed](#)]
12. Chen, J.; Ge, B.; Wang, Y.; Ye, Y.; Zeng, S.; Huang, Z.Q. Biochanin A promotes proliferation that involves feedback loop of microRNA-375 and estrogen receptor alpha in breast cancer cells. *Cell. Phys. Biochem.* **2015**, *2*, 639–646. [[CrossRef](#)] [[PubMed](#)]
13. Oh, M.; Choi, Y.H.; Choi, S.; Chung, H.; Kim, K.; Kim, S.I.; Kim, N.D. Anti-proliferating effects of ginsenoside Rh2 on MCF-7 human breast cancer cells. *Int. J. Oncol.* **1999**, *14*, 869–944. [[CrossRef](#)] [[PubMed](#)]

14. Park, H.M.; Kim, S.J.; Kim, J.S.; Kang, H.S. Reactive oxygen species mediated ginsenoside Rg3-and Rh2-induced apoptosis in hepatoma cells through mitochondrial signaling pathways. *Food Chem. Toxicol.* **2012**, *50*, 2736–2741. [[CrossRef](#)] [[PubMed](#)]
15. Wu, N.; Wu, G.C.; Hu, R.; Li, M.; Feng, H. Ginsenoside Rh2 inhibits glioma cell proliferation by targeting microRNA-128. *Acta Pharmacol. Sin.* **2011**, *32*, 345–353. [[CrossRef](#)] [[PubMed](#)]
16. Kim, H.S.; Lee, E.H.; Ko, S.R.; Choi, K.J.; Park, J.H.; Im, D.S. Effects of ginsenosides Rg3 and Rh2 on the proliferation of prostate cancer cells. *Arch. Pharmacol. Res.* **2004**, *27*, 429. [[CrossRef](#)]
17. Zhang, C.; Yu, H.; Hou, J. Effects of 20(S)-ginsenosideRh2 and 20(R)-ginsenoside Rh2 on proliferation and apoptosis of human lung adenocarcinoma A549 cells. *Chin. J. Chin. Mater. Med.* **2011**, *36*, 1670–1674.
18. Tan, J.W.; Kim, M.K. Neuro protective effects of Biochanin A against  $\beta$ -amyloid-induced neurotoxicity in PC12 cells via a mitochondrial-dependent apoptosis pathway. *Molecules* **2016**, *5*, 548. [[CrossRef](#)] [[PubMed](#)]
19. Quan, K.; Liu, Q.; Wan, J.Y.; Zhao, Y.J.; Guo, R.Z.; Alolga, R.N.; Qi, L.W. Rapid preparation of rare ginsenosides by acid transformation and their structure-activity relationships against cancer cells. *Sci. Rep.* **2015**, *5*, 8598. [[CrossRef](#)] [[PubMed](#)]
20. Hsu, J.T.; Hung, H.C.; Chen, C.J.; Hsu, W.L.; Ying, C. Effects of the dietary phytoestrogen biochanin A on cell growth in the mammary carcinoma cell line MCF-7. *J. Nutr. Biochem.* **1999**, *10*, 510–517. [[CrossRef](#)]
21. Moon, Y.J.; Shin, B.S.; An, G.; Morris, M.E. Morris, Biochanin A inhibits breast cancer tumor growth in a murine xenograft model. *Pharm. Res.* **2008**, *9*, 2158–2163. [[CrossRef](#)] [[PubMed](#)]
22. Choi, S.; Kim, T.W.; Singh, S.V. Ginsenoside Rh2-mediated G<sub>1</sub> phase cell cycle arrest in human breast cancer cells is caused by p15<sup>Ink4B</sup> and p27<sup>Kip1</sup>-dependent inhibition of cyclin-dependent kinases. *Pharm. Res.* **2009**, *26*, 2280–2288. [[CrossRef](#)] [[PubMed](#)]
23. Moon, Y.J.; Morris, M.E. Pharmacokinetics and bioavailability of the bioflavonoid biochanin A: Effects of quercetin and EGCG on biochanin A disposition in rats. *Mol. Pharm.* **2007**, *4*, 865–872. [[CrossRef](#)] [[PubMed](#)]
24. Xie, X.; Eberding, A.; Madera, C.; Fazli, L.; Jia, W.; Goldenberg, L.; Gleave, M.; Guns, E.S. Rh2 synergistically enhances paclitaxel or mitoxantrone in prostate cancer models. *J. Urol.* **2006**, *175*, 1926–1931. [[CrossRef](#)]
25. Xiao, P.; Zheng, B.W.; Sun, J.M.; Yang, J. Biochanin A induces anticancer effects in SK-Mel-28 human malignant melanoma cells via induction of apoptosis, inhibition of cell invasion and modulation of NF-kappa B and MAPK signaling pathways. *Oncol. Lett.* **2017**, *5*, 5989–5993. [[CrossRef](#)] [[PubMed](#)]
26. Zarubin, T.; Han, J. Activation and signaling of the p38 MAP kinase pathway. *Cell Res.* **2005**, *15*, 8–11. [[CrossRef](#)] [[PubMed](#)]
27. Yong, H.Y.; Koh, M.S.; Moon, A. The p38 MAPK inhibitors for the treatment of inflammatory diseases and cancer. *Expert Opin. Investig. Drug* **2009**, *18*, 1893–1905. [[CrossRef](#)] [[PubMed](#)]
28. Liu, Z.H.; Li, J.; Xia, J.; Jiang, R.; Zuo, G.W.; Li, X.P.; Chen, Y.; Xiong, W.; Chen, D.L. Ginsenoside 20(s)-Rh2 as potent natural histone deacetylase inhibitors suppressing the growth of human leukemia cells. *Chem. Biol. Interact.* **2015**, *5*, 227–234. [[CrossRef](#)] [[PubMed](#)]
29. Kim, Y.S.; Jin, S.H. Ginsenoside Rh2 induces apoptosis via activation of caspase-1 and -3 and up-regulation of Bax in human neuroblastoma. *Arch. Pharm. Res.* **2004**, *27*, 834–839. [[CrossRef](#)] [[PubMed](#)]
30. Kim, S.; Kim, A.K. Anti-breast cancer activity of Fine Black ginseng (*Panax ginseng* Meyer) and ginsenoside Rg5. *J. Ginseng Res.* **2015**, *39*, 125–134. [[CrossRef](#)] [[PubMed](#)]
31. Laptenko, O.; Prives, C. Transcriptional regulation by p53: One protein, many possibilities. *Cell Death Differ.* **2006**, *13*, 951–961. [[CrossRef](#)] [[PubMed](#)]
32. Brooks, C.L.; Gu, W. Ubiquitination, phosphorylation and acetylation: The molecular basis for p53 regulation. *Curr. Opin. Cell. Biol.* **2003**, *15*, 164–171. [[CrossRef](#)]
33. Felice, D.L.; Sun, J.; Liu, R.H. A modified methylene blue assay for accurate cell counting. *J. Funct. Foods* **2009**, *1*, 109–118. [[CrossRef](#)]
34. Jiang, X.; Li, T.; Liu, R.H. 2 $\alpha$ -Hydroxyursolic acid inhibited cell proliferation and induced apoptosis in MDA-MB-231 human breast cancer cells through the p38/MAPK signal transduction pathway. *J. Agric. Food Chem.* **2016**, *64*, 1806–1816. [[CrossRef](#)] [[PubMed](#)]
35. Chou, T.C. Drug combination studies and their synergy quantification using the Chou-Talalay method. *Cancer. Res.* **2010**, *70*, 440–446. [[CrossRef](#)] [[PubMed](#)]
36. Lee, J.H.; Kim, H.L.; Lee, M.H.; You, K.E.; Kwon, B.J.; Seo, H.J.; Park, J.C. Asiaticoside enhances normal human skin cell migration, attachment and growth in vitro wound healing model. *Phytomedicine* **2012**, *19*, 1223–1227. [[CrossRef](#)] [[PubMed](#)]

37. Tapia, P.A.; Argandona, F.; Palomino, W.A.; Devoto, L. Human chorionic gonadotropin (hCG) modulation of TIMP1 secretion by human endometrial stromal cells facilitates extravillous trophoblast invasion in vitro. *Hum. Reprod.* **2013**, *28*, 2215–2227. [[CrossRef](#)] [[PubMed](#)]
38. Yao, Y.; Zhu, Y.; Gao, Y.; Shi, Z.; Hu, Y.; Ren, G. Suppressive effects of saponin-enriched extracts from quinoa on 3T3-L1 adipocyte differentiation. *Food Funct.* **2015**, *6*, 3282–3290. [[CrossRef](#)] [[PubMed](#)]

**Sample Availability:** Samples of the compounds Combined Biochanin A and Ginsenoside Rh<sub>2</sub> are available from the authors.



© 2018 by the authors. Licensee MDPI, Basel, Switzerland. This article is an open access article distributed under the terms and conditions of the Creative Commons Attribution (CC BY) license (<http://creativecommons.org/licenses/by/4.0/>).